Applied and Computational Mechanics 4 (2010) 157–170

# Vibration analysis of tapered rotating composite beams using the hierarchical finite element

R. Ghayour[a], M. Ghayour[a,*], S. Ziaei-Rad[a]

[a] *Department of Mechanical Engineering, Isfahan University of Technology, Isfahan 84156-83111, Iran*

Received 21 June 2010; received in revised form 19 November 2010

**Abstract**

A hierarchical finite element model is presented for the flapwise bending vibration analysis of a tapered rotating multi-layered composite beam. The shear and rotary inertia effects are considered based on the higher shear deformation theory to derive the stiffness and mass matrices of a tapered-twisted rotating and composite beam element. Certain non-composite beams for which comparative results are available in the literature are used to illustrate the application of the proposed technique. Dimensionless parameters are identified from the equations of motion and the combined effects of the dimensionless parameters on the modal characteristics of the rotating composite beams are investigated through numerical studies. The results indicate that, compared with the conventional finite element method, the hierarchical finite element has the advantage of using fewer elements to obtain a better accuracy in the calculation of the vibration characteristics of rotating beams such as natural frequencies and mode shapes.


*Keywords:* vibration, tapered, composite beam, hierarchical FEM, rotating

## 1. Introduction

Rotating, tapered, laminated composite beams are basic structural components with applications in a variety of engineering structures such as airplane wings, helicopter blades, and turbine blades. The great possibilities provided by composite materials can be used to alter favorably the response characteristics of these structures. Due to their outstanding engineering properties, such as high stiffness-to-weight ratio, composite beam structures play a significant role in designing structures in which weight and strength are of primary importance. The behavior of composite beam structures can also be effectively and efficiently tailored by changing the lay-up parameters. It need be mentioned that it is far more difficult to analyze composite beams than it is to analyze their metallic counterparts.

An important element in the dynamic analysis of composite beams is the computation of their natural frequencies and mode shapes. This is important because composite beam structures often operate in complex environmental conditions and are frequently exposed to a variety of dynamic excitations. The characteristics of rotating flexible structures differ significantly from those of non-rotating ones. Centrifugal inertia force due to rotational motion causes variation in bending stiffness, which naturally results in variations in natural frequencies and mode shapes. Moreover, the stiffness property of composite structures can be easily modulated through changing their fiber orientation angles and number of layers.

The finite element method (FEM) is one of the most powerful numerical procedures for solving mathematical problems in engineering and physics. Nowadays, advanced formulations

*Corresponding author. Tel.: +983 113 915 247, e-mail: ghayour@cc.iut.ac.ir.

of the method such as the hierarchical FEM (HFEM) have been introduced. In conventional FEM, a beam element is modeled using two nodes at the end. Therefore, a large number of elements are needed to achieve an acceptable accuracy. In HFEM, however, a number of polynomial or trigonometric terms is introduced into the displacement and rotation function that yield higher degrees of freedom. Thus, the same accuracy can be achieved by using a much smaller number of elements. This results in rapid convergence.

Over the past four decades, investigators have carried out intensive studies on the dynamic analysis of rotating structures to improve their efficiency and dynamic characteristics. L. Chen and H. Chen [1] used the finite element model and incorporated the effect of rotation to study the transient response of a rotating blade of generally orthotropic materials. Sabuncu and Thomas [2] studied the vibration characteristics of pre-twisted aerofoil cross-section blade packets under rotating conditions. An improved two-node Timoshenko beam finite element was derived by Friedman and Kosmatka [3].The vibration of Timoshenko beams with discontinuities in cross-section was investigated by Farghaly and Gadelab [4, 5]. Corn *et al.* [6] derived finite element models through Guyan condensation method for the transverse vibration of short beams. Gupta and Rao [7] considered the finite element analysis of tapered and twisted Timoshenko beams. Gupta and Rao [8] applied finite element method for the analysis of rotating Timoshenko beams. A modeling method for the flapwise bending vibration analysis of a rotating multi-layered composite beam is presented in [9]. According to [10], a method is developed for dynamic response analysis of spinning tapered Timoshenko beams utilizing the finite element method. In [11], the effect of centrifugal forces on the eigenvalue solution obtained from using two different nonlinear finite element formulations is examined. In [12], the free and forced vibration of a rotating, pretwisted blade modeled as a laminated composite, hollow (single celled), uniform box-beam is studied. The structural model includes transverse shear flexibility, restrained warping, and centrifugal and Coriolis effects.

Most of these analytical works on composites are limited to static analysis. At the same time, the works on dynamic analysis of composite plates or beams have concentrated on uniform laminates. Tapered laminated beams have rarely ever been investigated despite their applications in important structures. Hoa and Ganesan [13] presented a review of recent developments in the analysis of tapered laminated composite structures with an emphasis on interlaminar stress analysis and delamination analysis. EL-Maksoud [14] studied the dynamic analysis of uniform and mid-plane tapered composite beams by using conventional and higher order finite element formulations. Borneman [15] presents a new dynamic finite element formulation for the free vibration of composite wings modeled as beam assemblies. W. Liu [16] studied the instability of tapered laminates under dynamic loading conditions. In [17], a dynamic finite element method for free vibration analysis of generally laminated composite beams is introduced on the basis of first order shear deformation theory. The influences of Poisson effect, couplings among extensional, bending and torsional deformations, shear deformation and rotary inertia are incorporated into the formulation. Conventional cubic Hermitian finite element formulation requires a large number of elements to obtain reasonably accurate results in the analysis of tapered laminated beams. Since the continuity of curvature at element interfaces cannot be guaranteed with the use of conventional formulation, the stress distribution across the thickness is not continuous at element interfaces. The material and geometric discontinuities at ply drop-off locations leads to additional discontinuities in stress distributions. As a result, efficient and accurate calculation of natural frequencies becomes very difficult.

In order to overcome these limitations, HFEM has been recently developed in many papers. Zabihollah [18] presents the vibration and buckling analysis of uniform and tapered composite beams using advanced finite element methods based on the classical laminate theory and the first shear deformation theory. Barrette [19] presented the vibration analysis of stiffened plates using hierarchical finite element with a set of local trigonometric interpolation functions. The functions have shown great numerical stability. Ramtekkar [20] used a mixed finite element formulation to calculate the natural frequencies of laminated beams. Nigam [21] used the hierarchical finite element method to investigate the static and dynamic responses of uniformly laminated composite beams. He used both polynomial and trigonometric functions and compared the convergences and accuracies to find that the latter outperforms the former. L. Chen [22] compared the conventional finite element with hierarchical finite element method in calculating natural frequencies. HFEM has the advantage of achieving a higher accuracy by using fewer elements.

In this paper, a hierarchical finite element technique is applied to find the natural frequencies and mode shapes of composite beams in the bending mode of vibration by taking into account the taper and the rotation simultaneously. The element mass and stiffness matrices are derived and the effects of offset, rotation, taper ratio, and shear deformation on the beam natural frequencies are investigated.

## 2. Derivation of the equations of motion

The configuration of a cantilever beam attached to a rotating rigid hub with the radius $r_e$ is shown in Figure 1. The elastic deformation of the beam is denoted by $\vec{u}$ in the Figure.

Neglecting $u$ along the beam in flapwise vibration analysis of rotating beams, the degrees of freedom for every point of the beam are $w(x,t)$ and $\theta(x,t)$.

The strain energy of a solid body in Cartesian coordinates can be expressed as:

$$\begin{aligned} U \;=\; & \frac{1}{2}\iiint (\sigma_x\varepsilon_x + \sigma_y\varepsilon_y + \sigma_z\varepsilon_z + \tau_{yz}\gamma_{yz} + \tau_{xz}\gamma_{xz} + \tau_{xy}\gamma_{xy})\,\mathrm{d}x\,\mathrm{d}y\,\mathrm{d}z - \\ & \frac{1}{2}\iint \left[N_x\left(\frac{\partial w}{\partial x}\right)^2 + 2N_{xy}\frac{\partial w}{\partial x}\frac{\partial w}{\partial y} + N_y\left(\frac{\partial w}{\partial y}\right)^2\right]\mathrm{d}x\,\mathrm{d}y. \end{aligned} \tag{1}$$

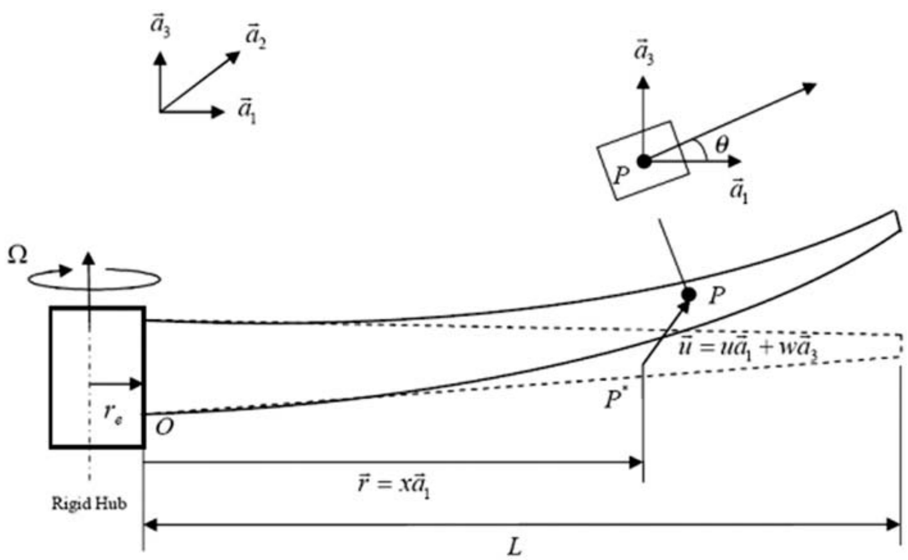


Fig. 1. Configuration of a rotating tapered cantilever beam

In rotating beam, the only load is the axial one due to the centrifugal force; thus

$$N_x = -\int_{r_e+x}^{r_e+L} \frac{\rho}{b}\Omega^2 x \,\mathrm{d}x = -\frac{\rho\Omega^2}{2b}\left((r_e+L)^2-(r_e+x)^2\right) = -\frac{\rho\Omega^2}{2b}\left(L^2-x^2+2r_e(L-x)\right). \tag{2}$$

In the above equation, $\rho$ is the mass per unit length of the beam and $b$ is the width of the rotating beam. The relation between stress and strain in the layers of a tapered laminated composite beam is

$$\left\{\begin{array}{c}\sigma_x\\ \sigma_y\\ \sigma_z\\ \tau_{yz}\\ \tau_{xz}\\ \tau_{xy}\end{array}\right\} = \left[\begin{array}{cccccc}\bar{C}_{11} & \bar{C}_{12} & \bar{C}_{13} & \bar{C}_{14} & \bar{C}_{15} & \bar{C}_{16}\\ & \bar{C}_{22} & \bar{C}_{23} & \bar{C}_{24} & \bar{C}_{25} & \bar{C}_{26}\\ & & \bar{C}_{33} & \bar{C}_{34} & \bar{C}_{35} & \bar{C}_{36}\\ & & & \bar{C}_{44} & \bar{C}_{45} & \bar{C}_{46}\\ & & & & \bar{C}_{55} & \bar{C}_{56}\\ sym & & & & & \bar{C}_{66}\end{array}\right] \left\{\begin{array}{c}\varepsilon_x\\ \varepsilon_y\\ \varepsilon_z\\ \gamma_{yz}\\ \gamma_{xz}\\ \gamma_{xy}\end{array}\right\}. \tag{3}$$

The shear stresses are related to the strains by

$$\left\{\begin{array}{c}\tau_{yz}\\ \tau_{xz}\end{array}\right\} = \left[\begin{array}{cccccc}\bar{C}_{14} & \bar{C}_{24} & \bar{C}_{34} & \bar{C}_{44} & \bar{C}_{45} & \bar{C}_{46}\\ \bar{C}_{15} & \bar{C}_{25} & \bar{C}_{35} & \bar{C}_{45} & \bar{C}_{55} & \bar{C}_{56}\end{array}\right] \left\{\begin{array}{c}\varepsilon_x\\ \varepsilon_y\\ \varepsilon_z\\ \gamma_{yz}\\ \gamma_{xz}\\ \gamma_{xy}\end{array}\right\}. \tag{4}$$

Since we assume that $w(x,y,z,t) = w^\circ(x,t)$, the strain $\varepsilon_z$ is zero. Therefore, the shear stresses are a function of five strains. If one neglects the inplane strains $\varepsilon_x$, $\varepsilon_y$ and $\gamma_{xy}$, the shear stresses relate to the shear strains by

$$\left\{\begin{array}{c}\tau_{yz}\\ \tau_{xz}\end{array}\right\} = k\left[\begin{array}{cc}\bar{C}_{44} & \bar{C}_{45}\\ \bar{C}_{45} & \bar{C}_{55}\end{array}\right]\left\{\begin{array}{c}\gamma_{yz}\\ \gamma_{xz}\end{array}\right\}. \tag{5}$$

The factor $k$ called the shear factor is equal to 5/6. Due to the first order shear theory for composite beam, the strains in the one dimension case are

$$\varepsilon_x = z\frac{\partial\theta}{\partial x}, \qquad \gamma_{xz} = \theta + \frac{\partial w}{\partial x}, \tag{6}$$

where $w, \theta$ are functions of $x, t$. Let us define

$$A_{55} = b\int_{-\frac{H}{2}}^{\frac{H}{2}} \bar{C}_{55}\,\mathrm{d}z, \qquad D_{11} = b\int_{-\frac{H}{2}}^{\frac{H}{2}} \bar{C}_{11} z^2\,\mathrm{d}z. \tag{7}$$

Using the above parameters, the strain energy of the tapered composite rotating beam will be

$$
\begin{aligned}
U = {} & \frac{1}{2}\iiint \left(\bar{C}_{11}\varepsilon_x^2 + k\bar{C}_{55}\gamma_{xz}^2\right)\,\mathrm{d}x\,\mathrm{d}y\,\mathrm{d}z + \\
& \frac{1}{2}\int \frac{\rho\Omega^2}{2}\left(L^2 - x^2 + 2r_e(L-x)\right)\left(\frac{\partial w}{\partial x}\right)^2 \mathrm{d}x = \\
& \frac{1}{2}\iiint \left(\bar{C}_{11}z^2\left(\frac{\partial\theta}{\partial x}\right)^2 + k\bar{C}_{55}\left(\theta + \frac{\partial w}{\partial x}\right)^2\right)\mathrm{d}x\,\mathrm{d}y\,\mathrm{d}z + \\
& \frac{1}{2}\int \frac{\rho\Omega^2}{2}\left(L^2 - x^2 + 2r_e(L-x)\right)\left(\frac{\partial w}{\partial x}\right)^2 \mathrm{d}x = \\
& \frac{1}{2}\iint b\left(\bar{C}_{11}z^2\left(\frac{\partial\theta}{\partial x}\right)^2 + k\bar{C}_{55}\left(\theta + \frac{\partial w}{\partial x}\right)^2\right)\mathrm{d}x\,\mathrm{d}z + \\
& \frac{1}{2}\int \frac{\rho\Omega^2}{2}\left(L^2 - x^2 + 2r_e(L-x)\right)\left(\frac{\partial w}{\partial x}\right)^2 \mathrm{d}x = \\
& \frac{1}{2}\int_0^L \left(D_{11}\left(\frac{\partial\theta}{\partial x}\right)^2 + kA_{55}\left(\theta + \frac{\partial w}{\partial x}\right)^2\right)\mathrm{d}x + \\
& \frac{1}{2}\int_0^L \frac{\rho\Omega^2}{2}\left(L^2 - x^2 + 2r_e(L-x)\right)\left(\frac{\partial w}{\partial x}\right)^2 \mathrm{d}x.
\end{aligned} \tag{8}
$$

The strain energy in its final form will be

$$
\begin{aligned}
U = {} & \frac{1}{2}\int_0^L kA_{55}\left(\frac{\partial w}{\partial x}\right)^2 \mathrm{d}x + \frac{1}{2}\int_0^L kA_{55}\left(\frac{\partial w}{\partial x}\right)\theta\,\mathrm{d}x + \\
& \frac{1}{2}\Omega^2 r_e\rho\int_0^L (L-x)\left(\frac{\partial w}{\partial x}\right)^2 \mathrm{d}x + \frac{1}{4}\Omega^2\rho\int_0^L (L^2 - x^2)\left(\frac{\partial w}{\partial x}\right)^2 \mathrm{d}x + \\
& \frac{1}{2}\int_0^L kA_{55}\theta\left(\frac{\partial w}{\partial x}\right)\mathrm{d}x + \frac{1}{2}\int_0^L D_{11}\left(\frac{\partial\theta}{\partial x}\right)^2 \mathrm{d}x + \frac{1}{2}\int_0^L kA_{55}\theta^2\,\mathrm{d}x.
\end{aligned} \tag{9}
$$

The kinetic energy of the tapered composite rotating beam can be written as

$$
\begin{aligned}
T = {} & \frac{1}{2}\iiint \rho'\left[\left(\frac{\partial u}{\partial t}\right)^2 + \left(\frac{\partial v}{\partial t}\right)^2 + \left(\frac{\partial w}{\partial t}\right)^2\right]\mathrm{d}x\,\mathrm{d}y\,\mathrm{d}z = \\
& \frac{1}{2}\int_0^L \rho\left(\frac{\partial w}{\partial t}\right)^2 \mathrm{d}x + \frac{1}{2}\int_0^L \rho\frac{I_2}{A}\left(\frac{\partial\theta}{\partial t}\right)^2 \mathrm{d}x,
\end{aligned} \tag{10}
$$

where $L$ denotes the length of the beam; $k$, the shear correction factor; $\theta$, the cross-section rotation angle; $\rho$, the mass per unit length of the beam; $b$, the width of the beam;$I_2$, the area moment of inertia in $\hat{a}_2$ axis; and A is the cross-section area of the beam. Also $A_{ij}$, $B_{ij}$ and $D_{ij}$ can be obtained by integrating the properties of the tapered composite beam layers (see [22]).

## 3. Hierarchical Finite element formulation

The finite element configuration of a rotating tapered cantilever beam is shown in Figure 2.

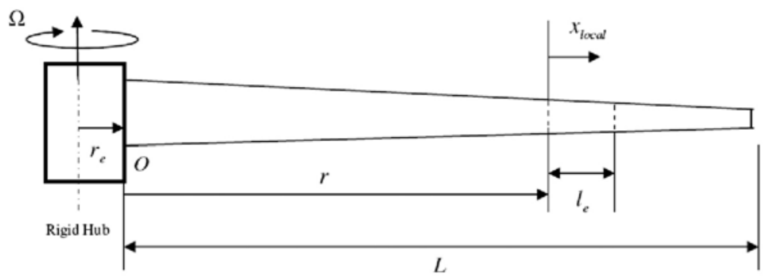


Fig. 2. Finite element configuration of a rotating tapered cantilever beam

For nodal analysis by HFEM, displacement and rotation functions are assumed to be as below:

$$
\begin{aligned}
w(x) &= \left(1-\frac{x}{l_e}\right)w_1 + \frac{x}{l_e}w_2 + \sum_{n=1}^{N} A_n \sin\frac{n\pi x}{l_e} = \\
& \begin{bmatrix} 1-\frac{x}{l_e} & \frac{x}{l_e} & \sin\frac{\pi x}{l_e} & \cdots & \sin\frac{N\pi x}{l_e} \end{bmatrix} \begin{Bmatrix} w_1 \\ w_2 \\ A_1 \\ \vdots \\ A_N \end{Bmatrix}, \\
\theta(x) &= \left(1-\frac{x}{l_e}\right)\theta_1 + \frac{x}{l_e}\theta_2 + \sum_{n=1}^{N} B_n \sin\frac{n\pi x}{l_e} = \\
& \begin{bmatrix} 1-\frac{x}{l_e} & \frac{x}{l_e} & \sin\frac{\pi x}{l_e} & \cdots & \sin\frac{N\pi x}{l_e} \end{bmatrix} \begin{Bmatrix} \theta_1 \\ \theta_2 \\ B_1 \\ \vdots \\ B_N \end{Bmatrix},
\end{aligned}
\tag{11}
$$

where $N$ is the number of hierarchical terms. In compact form

$$
w(x) = [N^w]\{W\}, \qquad \theta(x) = \left[N^\theta\right]\{\Theta\}, \tag{12}
$$

where $\{W\}$, $\{\Theta\}$ are the nodal displacements and rotations, respectively.

The expanded interpolation functions are:

$$
[N^w] = \left[N^\theta\right] = \begin{bmatrix} 1-\frac{x}{l_e} \\ \frac{x}{l_e} \\ \sin\frac{\pi x}{l_e} \\ \vdots \\ \sin\frac{n\pi x}{l_e} \end{bmatrix}_{(2+n)\times 1}. \tag{13}
$$

The following two notations are used:

$$
\left[N^{dw}\right] = \frac{\mathrm{d}\,[N^w]}{\mathrm{d}x}, \tag{14}
$$

$$
\left[N^{d\theta}\right] = \frac{\mathrm{d}\left[N^\theta\right]}{\mathrm{d}x}. \tag{15}
$$

The strain energy and kinetic energy of the system are:

$$U = \frac{1}{2}u^T [K] u, \qquad T = \frac{1}{2}\dot{u}^T [M] \dot{u}. \tag{16}$$

The components of the mass matrix are:

$$M_{11} = \int_0^{l_e} \rho [N^w]^T [N^w] \, \mathrm{d}x, \tag{17}$$

$$M_{22} = \int_0^{l_e} \rho \frac{I_2}{A} \left[N^\theta\right]^T \left[N^\theta\right] \mathrm{d}x. \tag{18}$$

For the stiffness matrix, the components are:

$$\begin{aligned} K_{11} = & \int_0^{l_e} kA_{55} \left[N^{dw}\right]^T \left[N^{dw}\right] \mathrm{d}x + \\ & \Omega^2 \left\{ r_e \rho \left( \int_0^{l_e} (L - (x + r)) \left[N^{dw}\right]^T \left[N^{dw}\right] \mathrm{d}x \right) + \right. \\ & \left. \frac{1}{2}\rho \left( \int_0^{l_e} (L^2 - (x+r)^2) \left[N^{dw}\right]^T \left[N^{dw}\right] \mathrm{d}x \right) \right\} \end{aligned} \tag{19}$$

$$K_{12} = \int_0^{l_e} kA_{55} \left[N^{dw}\right]^T \left[N^\theta\right] \mathrm{d}x \tag{20}$$

$$K_{21} = \int_0^{l_e} kA_{55} \left[N^{d\theta}\right]^T [N^w] \, \mathrm{d}x \tag{21}$$

$$K_{22} = \int_0^{l_e} D_{11} \left[N^{d\theta}\right]^T \left[N^{d\theta}\right] \mathrm{d}x + \int_0^{l_e} kA_{55} \left[N^\theta\right]^T \left[N^\theta\right] \mathrm{d}x. \tag{22}$$

By solving the following equation, the natural frequencies and the mode shapes of the composite rotating beam are obtained as:

$$\left| [K] - \omega^2 [M] \right| = 0, \tag{23}$$

where

$$[M] = \begin{bmatrix} M_{11} & 0 \\ 0 & M_{22} \end{bmatrix}, \tag{24}$$

$$[K] = \begin{bmatrix} K_{11} & K_{12} \\ K_{21} & K_{22} \end{bmatrix}. \tag{25}$$

## 4. Numerical results

Based on the above formulation, a finite element code was developed for the rotating composite beams. In what follows, the code will be verified using the data available in the literature.

### *4.1. Free vibration of a non-rotating simply-supported composite beam*

In order to validate the present dynamic stiffness formulation, a symmetric cross-ply $[90°/0°/0°/90°]$ laminated beam with the simply-supported boundary condition is considered. This example is selected due to the comparative results already available in [23]. The properties of the laminated beam are presented in Table 1.

Table 1. Material properties of the laminated beam

| $E_1$ (GPa) | $E_2$ (GPa) | $G_{12}$ (GPa) | $G_{13}$ (GPa) | $G_{23}$ (GPa) | $\nu_{12}$ | $\rho$ (Kg/m$^3$) | $L$ (m) | $b$ (m) | $h$ (m) |
|---|---|---|---|---|---|---|---|---|---|
| 241.5 | 18.98 | 5.18 | 5.18 | 3.45 | 0.24 | 2 015 | 6.35 | 0.279 4 | 0.279 4 |

The first six natural frequencies of the simply-supported laminated beam for the first six modes are calculated using the HFEM presented in Table 2. The number of hierarchical elements used in the calculation is 100. Table 2 also shows a comparison of the results with those of [23] and the Abaqus solutions in [24]. It can be observed that the present results are in good agreement with those presented in [23, 24].

Table 2. Natural frequencies (in Hz) of simply-supported laminated beam

| **Mode** | $\omega$ **Ref [23]** | $\omega$ **Abaqus [24]** | $\omega$ **Present Study** |
|---|---|---|---|
| 1 | 14.9 | 14.95 | 15.00 |
| 2 | 58.1 | 57.6 | 58.1 |
| 3 | 124.5 | 122.8 | 124.7 |
| 4 | 208.6 | 204.2 | 208.8 |
| 5 | 304.8 | 296.6 | 305.0 |
| 6 | 408.9 | 396.2 | 409.2 |

## 4.2. *Vibration of a rotating fixed-free composite beam using HFEM*

In this example, a tapered composite beam is considered and the results are presented for both stationary and rotating cases. To obtain the numerical results, the composite beams consisting of 4 skew symmetric fiber orientation layers $[0°/90°/-90°/0°]$ are considered in this example. All the layers have identical thicknesses and the composite beams are made of graphite-epoxy. The beam aspect ratio is assumed to be $L/h = 10$, where $L$ is the length of the beam and $h$ denotes beam width and thickness. The material properties of the graphite-epoxy are given in Table 3.

Table 3. Material properties of the graphite- epoxy used for the composite beams

| $E_1$ (GPa) | $E_2$ (GPa) | $E_3$ (GPa) | $G_{12}$ (GPa) | $G_{13}$ (GPa) | $G_{23}$ (GPa) | $\nu_{13}$ | $k$ |
|---|---|---|---|---|---|---|---|
| 145 | 9.6 | 9.6 | 4.1 | 4.1 | 3.4 | 0.3 | 5/6 |

To check the accuracy of the modeling method proposed in this study, the numerical results obtained are compared with those presented in [9] and those obtained from the commercial program Ansys. The number of hierarchical terms is set to 100.

In Table 4, $\bar{\omega}$ denotes the dimensionless natural frequencies (i.e. natural frequencies multiplied by $T \equiv \sqrt{\frac{\rho L^4}{D}}$, where $D$ denotes the value of $D_{11}$ when all the layer angles are zero). For the composite beam with rotation, a constant $\gamma = T\Omega$ is defined where $\Omega$ is the angular speed of the rigid hub.

Table 4. Comparison of the first five dimensionless natural frequencies for a stationary composite beam

| **Mode** | $\bar{\omega}$ **Ref [25]** | $\bar{\omega}$ **Ref [9]** | $\bar{\omega}$ **Present Study** |
|---|---|---|---|
| 1 | 3.073 | 3.064 | 3.062 |
| 2 | 14.44 | 14.36 | 14.18 |
| 3 | 31.75 | 31.40 | 30.91 |
| 4 | 49.68 | 48.87 | 47.98 |
| 5 | 66.23 | 66.24 | 65.15 |

Table 5. Comparison of the first three dimensionless natural frequencies for the rotating composite beam

| $\gamma$ | **Mode** | **Ref [9]** | **ANSYS [9]** | **Present Study** |
|---|---|---|---|---|
| 0 | 1 | 3.067 | 3.06 | 3.062 |
| | 2 | 14.359 | 14.172 | 14.183 |
| | 3 | 31.397 | 30.878 | 30.908 |
| 10 | 1 | 10.698 | 10.63 | 10.62 |
| | 2 | 28.802 | 28.525 | 28.478 |
| | 3 | 52.397 | 51.729 | 51.696 |
| 20 | 1 | 20.522 | 20.356 | 20.324 |
| | 2 | 51.492 | 51.05 | 50.97 |
| | 3 | 86.791 | 85.786 | 85.779 |

### 4.3. *Vibration of a rotating tapered composite beam using HFEM*

A tapered composite beam is made of NCT301 graphite-epoxy is shown in Figure 3. Its mechanical properties are shown in Table 6.

Table 6. Mechanical properties of NCT301 graphite-epoxy

| $E_1$ (GPa) | $E_2, E_3$ (GPa) | $\nu_{21}, \nu_{31}$ | $\nu_{23}$ | $G_{12}, G_{13}$ (GPa) | $G_{23}$ (GPa) | $\rho$ (Kg/m$^3$) |
|---|---|---|---|---|---|---|
| 144 | 12.14 | 0.017 | 0.458 | 4.48 | 3.2 | 1 660.8 |


Fig. 3. Free-fixed tapered composite beam

The geometric properties of the beam are: length, $L = 0.304\,8$ m; and individual ply thickness, $t = 0.000\,152\,4$ m. There are 32 plies at the left end and 30 plies at the right end. The configuration of both ends are $[(0/90)_8]_S$ and $[(0/90)_7/0]_S$, respectively.

The parameters related to the tapered properties of the composite beam are:

$$A_{55} = 18\,726\,912 - 3\,200\,000x \text{ (N} \cdot \text{m}^{-1}\text{)},$$
$$D_{11} = 817.122 - 490.366x + 95.509\,7x^2 - 1.015\,15x^3 \text{ (N} \cdot \text{m)},$$
$$D = -12.044x^3 + 176.19x^2 - 859.2x + 1\,396.6 \text{ (N} \cdot \text{m)}.$$

Table 7 presents the first four natural frequencies of the non-rotating tapered composite beam with simply supported boundary conditions. This sub case was selected to further validate the proposed method and the associated code developed. The results calculated by using the code are compared with those reported in [22], which have been obtained by using the Ritz method. It is noteworthy that there is no exact solution for the tapered composite beams.

Table 7. Natural frequencies of non-rotation simply supported tapered composite beam

| Mode | $\omega$ (Rad/s) Using Ritz method [22] | $\omega$ (Rad/s) Present Study |
|---|---|---|
| 1 | **1 031.89** | **1 063.99** |
| 2 | **4 096.45** | **4 219.83** |
| 3 | **9 101.65** | **9 363.77** |
| 4 | **15 906.20** | **16 337.24** |

The first five natural frequencies of the rotating fixed-free tapered beam are presented in Table 8. Natural frequencies are calculated for the following three different conditions: 1) non-rotating ($\gamma = 0$), and the rotating cases ($\gamma = 10$, $\gamma = 20$).

Table 8. Natural frequencies of fixed-free tapered composite beam (Rad/Sec)

| $\gamma$ | mode | $m = 10$ $n = 0$ | $m = 10$ $n = 1$ | $m = 10$ $n = 2$ | $m = 10$ $n = 3$ | $m = 10$ $n = 4$ | $m = 10$ $n = 5$ | $m = 10$ $n = 6$ | $m = 10$ $n = 7$ | $m = 10$ $n = 8$ |
|---|---|---|---|---|---|---|---|---|---|---|
| 0 | 1 | 606.93 | 389.38 | 388.78 | 385.78 | 385.744 24 | 385.322 85 | 385.317 17 | 385.204 49 | 385.202 9 |
| | 2 | 3 816.74 | 2 427.84 | 2 416.83 | 2 398.91 | 2 398.178 9 | 2 395.667 3 | 2 395.527 4 | 2 394.855 3 | 2 394.812 7 |
| | 3 | 10 822.77 | 6 745.77 | 6 680.89 | 6 635.06 | 6 630.660 1 | 6 624.252 2 | 6 623.393 7 | 6 621.676 9 | 6 621.410 5 |
| | 4 | 21 652.32 | 13 082.52 | 12 855.53 | 12 778.09 | 12 762.989 | 12 752.195 | 12 749.229 | 12 746.331 | 12 745.404 |
| | 5 | 36 727.51 | 21 368.42 | 20 774.29 | 20 671.47 | 20 633.429 | 20 619.137 | 20 611.658 | 20 607.808 | 20 605.465 |
| 10 | 1 | 1 649.750 4 | 1 566.372 | 1 565.428 5 | 1 564.276 7 | 1 564.206 1 | 1 564.044 6 | 1 564.030 4 | 1 563.987 2 | 1 563.982 7 |
| | 2 | 5 288.555 7 | 4 381.221 8 | 4 373.395 | 4 362.888 | 4 362.341 1 | 4 360.875 7 | 4 360.768 8 | 4 360.377 3 | 4 360.344 1 |
| | 3 | 12 428.722 | 9 037.720 1 | 8 986.745 4 | 8 950.758 | 8 947.272 8 | 8 942.261 3 | 8 941.577 9 | 8 940.237 | 8 940.024 2 |
| | 4 | 23 387.187 | 15 636.352 | 15 442.359 | 15 374.617 | 15 361.704 | 15 352.297 | 15 349.757 | 15 347.235 | 15 346.441 |
| | 5 | 38 570.16 | 24 105.481 | 23 570.153 | 23 475.037 | 23 440.807 | 23 427.634 | 23 420.904 | 23 417.361 | 23 415.252 |
| 20 | 1 | 3 058.334 7 | 2 994.325 7 | 2 992.050 1 | 2 990.948 3 | 2 990.773 4 | 2 990.618 4 | 2 990.582 4 | 2 990.541 | 2 990.529 5 |
| | 2 | 8 221.556 3 | 7 621.025 2 | 7 612.304 4 | 7 604.968 | 7 604.328 4 | 7 603.309 1 | 7 603.180 4 | 7 602.908 4 | 7 602.867 8 |
| | 3 | 16 241.623 | 13 605.421 | 13 561.763 | 13 533.673 | 13 530.646 | 13 526.756 | 13 526.156 | 13 525.117 | 13 524.93 |
| | 4 | 27 874.147 | 21 320.01 | 21 156.104 | 21 099.273 | 21 088.355 | 21 080.511 | 21 078.357 | 21 076.26 | 21 075.585 |
| | 5 | 43 573.883 | 30 681.784 | 30 217.059 | 30 133.062 | 30 103.445 | 30 091.893 | 30 086.066 | 30 082.969 | 30 081.141 |

Parameter $D$ is defined t as in Table 5; however it is here defined at the root place (i.e., at $x = 0$). In this Table, $m$ denotes the number of elements and $n$ is the number of trigonometric terms. The table indicates that by increasing the trigonometric terms, the accuracy of the solutions is enhanced. This is more apparent for higher modes. It is noticeable that for the first natural frequency of the non-rotating beam, even with 2 000 conventional elements, the results are different from those obtained with $m = 10$ and $n = 8$. The Table also shows that the natural frequencies of the beam increase with beam rotating speed.

Figures 4 to 7 depict the first four natural frequencies of the rotating tapered composite beam versus the number of elements.

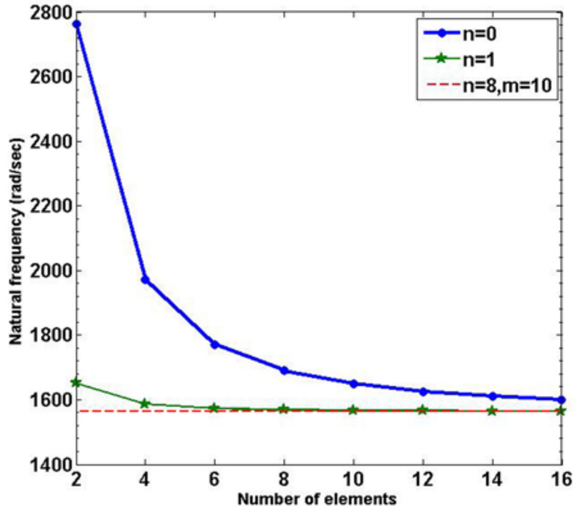


Fig. 4. The first natural frequency of rotating fixed-free tapered composite beam ($\gamma = 10$)

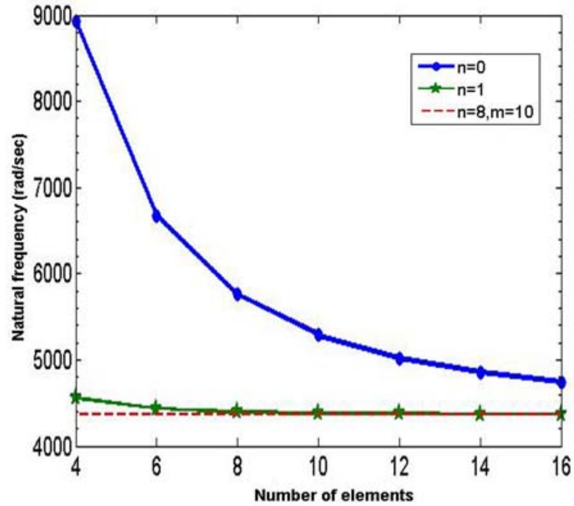


Fig. 5. The second natural frequency of rotating fixed-free tapered composite beam ($\gamma = 10$)

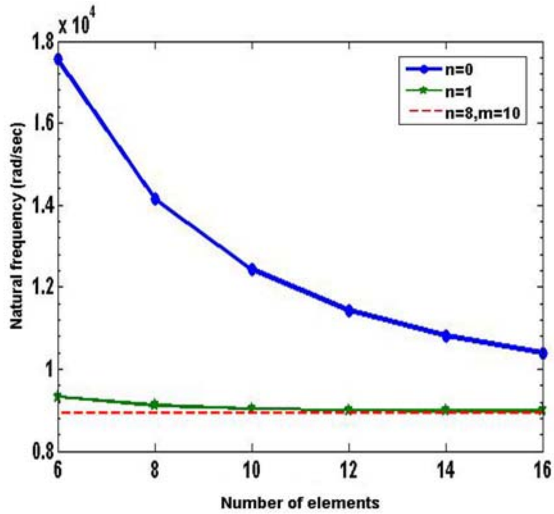


Fig. 6. The third natural frequency of rotating fixed-free tapered composite beam ($\gamma = 10$)

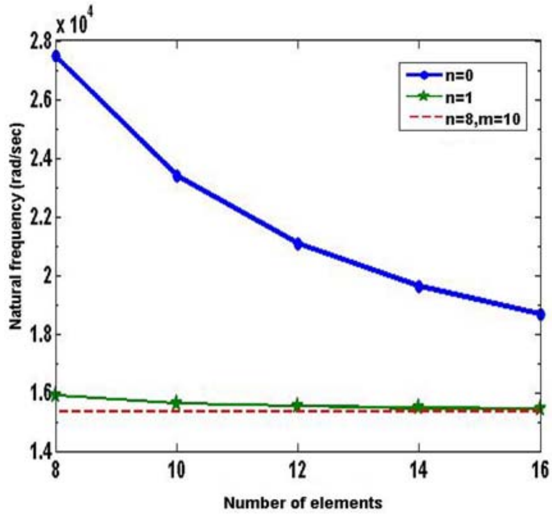


Fig. 7. The fourth natural frequency of rotating fixed-free tapered composite beam ($\gamma = 10$)

In each Figure, the results obtained from the conventional finite element code are compared with those of the HFEM with one trigonometric term (i.e. $n = 1$). The dashed line in each Figure is calculated for $m = 10$ and $n = 8$, which is assumed to be the exact solution.

The first five modes of vibrations are shown in Figures 8(a)–(e). In these Figures, the solid lines represent the mode shapes of the non-rotating beam while the dashed lines represent the same for the rotating beam. The Figures indicate that the deflection shape of a rotating beam is smaller than that of a non-rotating beam due to the centrifugal forces.

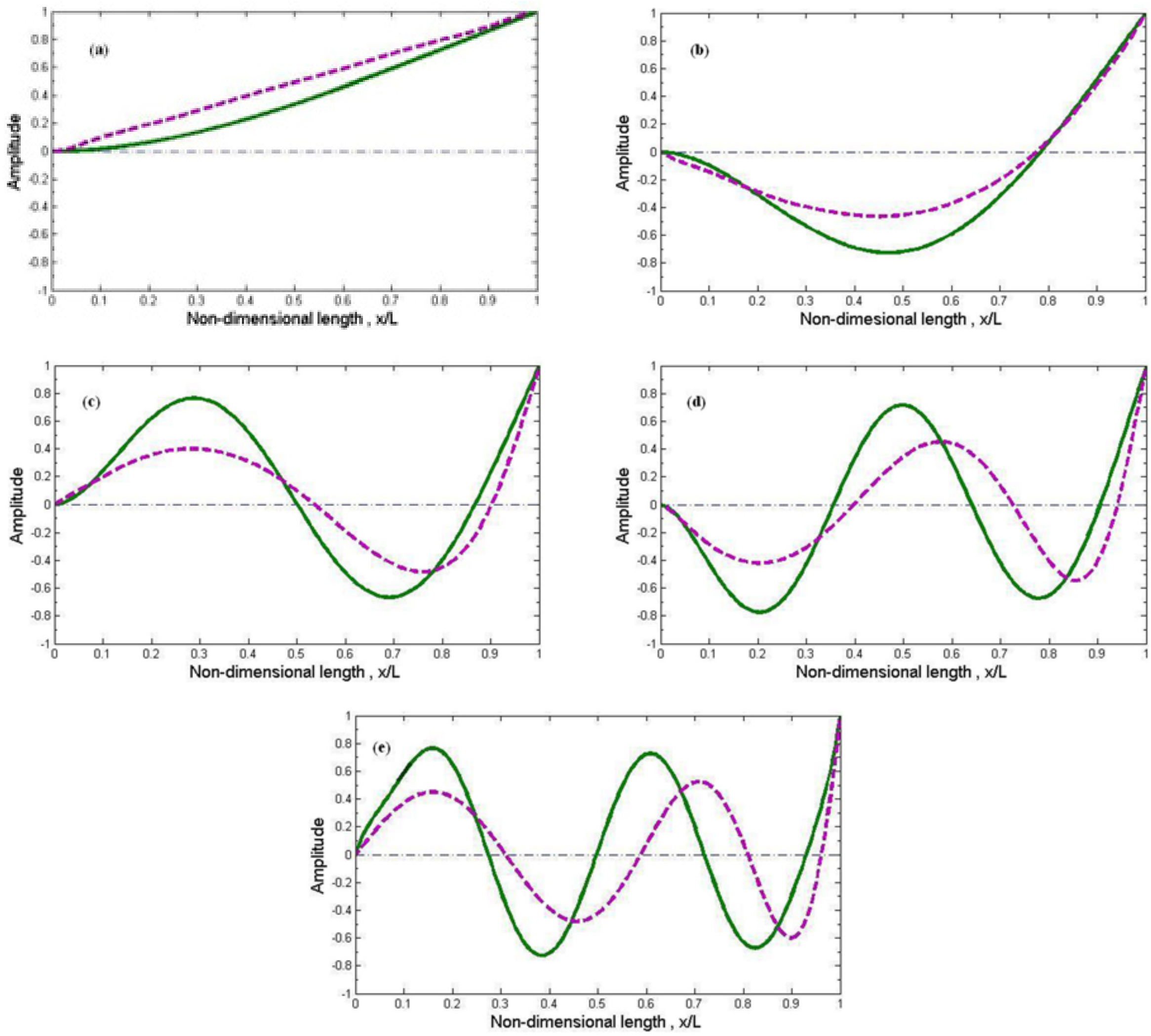


— $\gamma = 0$; ---- $\gamma = 100$ Mode number, $\omega_{\gamma=100}$: (a) 1, 14 448.63; (b) 2, 35 437.36; (c) 3, 56 618.81; (d) 4, 79 044.43; (e) 5, 102 898.88

Fig. 8. Mode shape of rotating fixed-free tapered composite beam

## 5. Conclusions

A hieratical finite element formulation was developed for the vibration analysis of rotating tapered composite beams. The taper angle of the composite beam changes not only its geometric properties but also the stiffness of the oblique plies. This causes the mechanical behavior of the tapered composite beam to be different from that of the uniform beam. Therefore, it is necessary to consider the effect of the laminate stiffness of the composite beam caused by the taper angle.

Based on the proposed formulation, the mass and stiffness matrices of a tapered composite rotating beam element were developed for the eigenvalue analysis of rotating, doubly tapered beams. The element was found to give reasonably accurate results. The consideration of shear deformation was found to reduce the values of the higher natural frequencies of beam vibration.

The results indicate that the hieratical finite element formulation uses fewer elements to obtain accurate results, which, in turn, leads to less costly computational processes. Comparison with available data reveals that the method is accurate and can be used for a large class of rotating beams.

## References

[1] Chen, L. W., Chen, H. K., Transient responses of a pre-twisted rotating blade of general orthotropy, Finite Elements Anal. Des. (13) (1993) 285–298.

[2] Sabuncu, M., Thomas, J., Vibration characteristics of pretwisted aerofoil cross-section blade packets under rotating conditions, American Institute of Aeronautics and Astronautics Journal (30) (1992) 241–250.

[3] Friedman, Z., Kosmatka, J.B., An improved two-node Timoshenko beam finite element, Computers and Structures (47) (1993) 473–481.

[4] Farghaly, S. H., Vibration and stability analysis of Timoshenko beams with discontinuities in cross-section, Journal of Sound and vibration (174) (1994) 591–605.

[5] Farghaly, S. H., Gadelrab, R.M., Free vibration of a stepped composite Timoshenko cantilever beam, Journal of Sound and vibration (187) (1995) 886–896.

[6] Corn, S., Buhaddi, N., Piranda, J., Transverse vibrations of short beams: finite element models obtained by a condensation method, Journal of Sound and vibration (201) (1997) 353–363.

[7] Gupta, R. S., Rao, S. S., Finite element eigenvalue analysis of tapered and twisted Timoshenko beams, Journal of Sound and vibration (56) (1978) 187–200.

[8] Gupta, R. S., Rao, S. S., Finite element vibration analysis of rotating Timoshenko beams. J. Sound Vibration 242(1) (2001) 103–24.

[9] Yoo, H. H., Lee, S. H., Shin, S. H., Flapwise bending vibration analysis of rotating multi-layered composite beams, Journal of Sound and Vibration (286) (2005) 745–761.

[10] Bazoune, A., Khulief, Y.A., Stephen, N. G., Mohiuddin, M. A., Dynamic response of spinning tapered Timoshenko beams using modal reduction, Finite Elements in Analysis and Design (37) (2001) 199–219.

[11] Maqueda, L. G., Bauchau, O. A., Shabana, A. A., Effect of the centrifugal forces on the finite element eigenvalue solution of a rotating blade: a comparative study, Springer Science Multibody Syst Dyn (19) (2008) 281–302.

[12] Chandiramania, N. K., Shetea, C. D., Librescu, L. I., Vibration of higher-order-shearable pretwisted rotating composite blades, International Journal of Mechanical Sciences (45) (2003) 2 017–2 041.

[13] He, K., Hoa, S. V., Ganesan, R., The study of tapered laminated composite structures: a review, composites science and technology 60 (14) (2000) 2 643–2 657.

[14] EL-Maksoud Abd, Mohamed, A., Dynamic analysis and Buckling of variable thickness laminated composite beams using conventional and advanced finite element formulation, M.A.Sc. Thesis, Concordia University, 2000.

[15] Borneman, S. R., A New Dynamic Finite Element Formulation with Application To Composite Aircraft Wings, M.A.Sc. Thesis, Ryerson University, 2004.

[16] Liu, W., Dynamic instability analysis of tapered composite plates using Ritz and finite element methods, M.A.Sc. Thesis, Concordia University, 2005.

[17] Jun, L., Hongxing, H., Rongying, S. H., Dynamic finite element method for generally laminated composite beams, International Journal of Mechanical Sciences, (50) (2008) 466–480.

[18] Zabihollah, A., Vibration analysis of tapered composite beams using a higher-order finite element formulations, composite structures, (77) (2007) 306–318.

[19] Barrette, M., Berry, A., Vibration of stiffened plates using Hierarchical Trigonometric Functions, Journal of Sound and Vibration, 235(5) (2000) 727–747.

[20] Ramtekkar, G. S., Desai, Y. M. Natural Vibration of Laminated Composite Beams by Mixed Finite Element Modeling, Journal of Sound and Vibration, Vol. 257(4) (2002) 635–651.

[21] Nigan, Amit, Dynamic Analysis of Composite Beams using Hierarchical Finite Element Meyhod, M.A.Sc. Thesis Concordia University, 2002.

[22] Chen, L., Free Vibration Analysis of Tapered Composite Beams using Hierarchical Finite Element Method, M.A.Sc. Thesis Concordia University, 2004.

[23] Jun, L., Hongxing, H., Rongying, S., Dynamic stiffness analysis for free vibrations of axially loaded laminated composite beams, Composite Structures (84) (2008) 87–98.

[24] Karama, M., Abou Harb, B., Mistou, S., Caperaa, S., Bending, buckling and free vibration of laminated composite with a transverse shear stress continuity model, Composite (29) (1998) 223–234.

[25] Singh, M., Abdelnaser, A., Random response of symmetric cross-ply composite beams with arbitrary boundary conditions, AIAA Journal (30) (1992) 201–210.